Selective agonism of GPR34 stimulates microglial uptake and clearance of amyloid β fibrils

Hayato Etani[1,11], Sho Takatori[1,11], Wenbo Wang[1], Jumpei Omi[2], Aika Akahori[1], Hirotaka Watanabe[3,4], Iki Sonn[3], Hideyuki Okano[3,4], Norikazu Hara[5], Mai Hasegawa[5], Akinori Miyashita[5], Masataka Kikuchi[5], Takeshi Ikeuchi[5], Maho Morishima[6], Yuko Saito[6], Shigeo Murayama[6], Takashi Saito[7], Takaomi C Saido[8], Toshiyuki Takai[9], Tomohiko Ohwada[10], Junken Aoki[2] and Taisuke Tomita[1]

1. Laboratory of Neuropathology and Neuroscience, Graduate School of Pharmaceutical Sciences, The University of Tokyo, 7-3-1 Hongo, Bunkyo-ku, Tokyo 113-0033, Japan
2. Department of Health Chemistry, Graduate School of Pharmaceutical Sciences, The University of Tokyo, Tokyo 113-0033, Japan
3. Department of Physiology, Keio University School of Medicine, Tokyo, 160-8582, Japan
4. Keio University Regenerative Medicine Research Center, Kanagawa, 210-0821, Japan
5. Department of Molecular Genetics, Brain Research Institute, Niigata University, Niigata, Japan.
6. Department of Neuropathology (the Brain Bank for Aging Research), Tokyo Metropolitan Institute for Geriatrics and Gerontology, Tokyo 173-0015, Japan.
7. Department of Neurocognitive Science, Institute of Brain Science, Nagoya City University Graduate School of Medical Science, 1 Kawasumi, Mizuho-cho, Mizuho-ku, Nagoya, Aichi 467-8601, Japan

8. Laboratory for Proteolytic Neuroscience, RIKEN Center for Brain Science, 2-1 Hirosawa, Wako, Saitama 351-0198, Japan
9. Department of Experimental Immunology, Institute of Development, Aging and Cancer, Tohoku University, 4-1 Seiryo, Sendai 980-8575, Japan.
10. Department of Organic and Medicinal Chemistry, Graduate School of Pharmaceutical Sciences, The University of Tokyo, Tokyo 113-0033, Japan
11. These authors contributed equally to this work.

Correspondence: Taisuke Tomita (taisuke@mol.f.u-tokyo.ac.jp)

Classification: Biological Sciences (Immunology and Inflammation; Neuroscience)

Keywords: Alzheimer disease, Amyloid-β, Microglia, GPR34

Abstract

Microglia, the primary immune cells of the central nervous system, play a crucial role in maintaining brain homeostasis through phagocytosis of various substrates, including amyloid-β (Aβ) fibrils, a hallmark of Alzheimer disease (AD) pathology. However, the molecular mechanisms regulating microglial Aβ uptake remain poorly understood. Here, we identified GPR34, a Gi/o-coupled receptor highly expressed in microglia, as a novel regulator of fibrillar Aβ phagocytosis. Treatment with a selective GPR34 agonist, M1, specifically enhanced uptake of Aβ fibrils, but not its monomer or oligomer, in both mouse and human microglia. Mechanistically, M1 reduced intracellular cAMP levels, which inversely correlated with Aβ uptake activity. Importantly, a single intrahippocampal injection of M1 in an AD mouse model significantly increased microglial Aβ uptake in vivo. Furthermore, single-nucleus RNA-sequencing analysis of Japanese AD patient samples revealed a significant reduction of GPR34 expression in microglia from AD patients compared to controls. We also observed an age-dependent decline in microglial GPR34 expression in both human and mouse datasets, suggesting a potential contribution of GPR34 downregulation to age-related Aβ accumulation and AD risk. Collectively, our findings identify GPR34 as a promising target for modulating microglial Aβ clearance and highlight the therapeutic potential of GPR34 agonists in AD.

Significance statement

Alzheimer disease (AD) is characterized by amyloid-β (Aβ) accumulation in the brain. Microglia, the brain's immune cells, play a crucial role in the metabolism of Aβ. We discovered that activating the microglial receptor GPR34 with a selective agonist enhances the phagocytosis of Aβ fibrils, a key pathogenic form of Aβ. Importantly,

GPR34 expression decreases with aging and AD progression, potentially contributing to impaired Aβ clearance. Our findings highlight GPR34 as a promising therapeutic target for AD, as boosting its activity could promote Aβ clearance and slow disease progression. This study provides valuable insights into microglial function in AD and offers a novel strategy for developing disease-modifying therapies.

Introduction

Imbalances in the production and clearance of amyloid-β (Aβ) peptides in the brain are central to the pathogenesis of Alzheimer disease (AD). For example, mutations elevating Aβ production or aggregation are implicated in familial AD (1). Conversely, the *APP* A673T variant, which is associated with lower Aβ levels, significantly reduces the risk of late-onset AD (2). In addition, recently approved anti-Aβ antibodies have shown efficacy in slowing cognitive decline and disease progression in AD patients by improving Aβ clearance (3, 4). Taken together, these findings position cerebral Aβ levels as a critical determinant of AD pathogenesis and progression, and highlight drugs that promote Aβ clearance as potential preventive and disease-modifying therapies. However, the precise mechanisms underlying Aβ clearance remain to be elucidated.

As resident immune cells of the central nervous system (CNS), microglia phagocytose and degrade extracellular Aβ species. Recent genetic analyses have identified numerous genetic risk factors for AD, many of which are found in genes that are highly or specifically expressed in microglia (5, 6). Among these genes, *TREM2* encodes a microglial Aβ receptor, and its rare hypomorphic variant significantly increases AD risk (7, 8). *Trem2* deficiency in AD mouse models exacerbates Aβ deposition (9–11), highlighting the pathologically important role of TREM2-mediated Aβ clearance. Thus, impairments in microglial clearance pathways may promote AD pathogenesis, whereas enhancing microglial phagocytic activity holds promise for preventing or slowing disease progression. Therapeutics aimed at activating Aβ clearance by microglia may be beneficial in AD.

G-protein coupled receptor 34 (GPR34) is a Gi/o-coupled receptor highly expressed in mononuclear cells of the immune system. In the CNS, GPR34 is specifically expressed

95 in microglia, especially in the homeostatic state (12, 13). Together with P2RY10 and
96 GPR174, GPR34 comprises the lysophosphatidylserine (LysoPS) receptor family (14, 15).
97 Uniquely within this receptor family, GPR34 exhibits selectivity for LysoPS species with
98 a fatty acid at the *sn*-2 position (16–19). While GPR34 is involved in various
99 immunomodulatory functions (20–22), another study highlights its importance in the
100 regulation of phagocytosis in microglia (23). Regarding pathological associations,
101 GPR34 is involved in the neuropathic pain after nerve injury (24). However, the
102 relationship between GPR34 and AD pathology remains largely unknown, in particular
103 whether GPR34 contributes to Aβ clearance by microglia.

104 In this study, we report that activating GPR34 with our recently developed selective
105 agonist M1 (referred to as compound **14** in (18)) enhances microglial phagocytosis of Aβ.
106 In mouse primary microglia, M1 specifically increased uptake of Aβ fibrils without
107 affecting Aβ monomers or oligomers. The underlying mechanism involves the
108 suppression of cyclic AMP (cAMP) levels in microglia. Enhancement of Aβ phagocytosis
109 by M1 was also observed in human microglia-like cells and further validated *in vivo* using
110 an AD mouse model. In addition, we found that expression of GPR34 decreases with age
111 and shows its reduction in human AD brains correlating with amyloid deposition. Taken
112 together, these results demonstrate that GPR34 activation promotes microglial clearance
113 of Aβ fibrils, suggesting that age-related GPR34 reductions may contribute to AD
114 pathogenesis.

115

116 **Results**

117 *Selective agonism of GPR34 specifically increases microglial uptake of Aβ fibrils*

118 To investigate the effect of the GPR34 agonist M1 (Fig. 1*A*) on microglial uptake of

119 Aβ, we adapted a flow cytometry-based assay previously described by Mandrekar *et al.*
120 (25). This assay measures cellular fluorescence derived from fluorophore-conjugated,
121 internalized Aβ fibrils (fAβ). Exposing murine primary microglia to fluorescent fAβ for
122 3 hours resulted in an elevated fluorescence profile, which typically appeared as a broad
123 peak or, under certain experimental conditions, as two distinct peaks (Fig. 1*B*). The peak
124 with higher fluorescence intensity corresponds to cells that have phagocytosed high-
125 molecular-weight Aβ aggregates, consistent with the previous findings (25). Our analysis
126 focused on both the proportion and the mean fluorescence intensity (MFI) of cells
127 exhibiting this higher fluorescence. We found that treatment with M1 at concentrations
128 above 10 nM led to an approximate 35% increase in the MFI of $fA\beta^+$ cells (Fig. 1 *B* and
129 *C*), without affecting the proportion of $fA\beta^+$ cells (*SI Appendix*, Fig. S1 *A–C*). This
130 suggests that M1 increases the quantity of fAβ engulfed by individual microglial cells.
131 The positive effect of M1 was not observed at concentrations below 1 nM, consistent with
132 the previously reported EC_{50} value of 5 nM for M1 (18). Furthermore, the effect was
133 evident as early as 1.5 hours after exposure to M1 and persisted for at least 7.5 hours (Fig.
134 1*D*). To confirm that the observed effect is mediated through GPR34, we assessed the
135 impact of M1 in *Gpr34* knockdown cells. Two independent siRNAs targeting *Gpr34*
136 resulted in a substantial reduction in *Gpr34* expression (Fig. 1*E*). Notably, *Gpr34*
137 knockdown itself led to a significant decrease or a trend towards reduced uptake of fAβ
138 (Fig. 1*F*), suggesting that GPR34 positively regulates fAβ phagocytosis. Furthermore,
139 *Gpr34* knockdown abrogated the M1-induced increase in fAβ uptake (Fig. 1*F*), indicating
140 that GPR34 is indeed the target of M1.

141 Soluble Aβ species are taken up differently than fAβ, through non-phagocytic
142 mechanisms such as macropinocytosis (25). Therefore, we examined the effects of M1

143 on the uptake of Aβ monomer and oligomer. At any concentrations, M1 did not
144 significantly alter the MFI of fluorescence-positive cells for these soluble Aβ (Fig. 1*G*, *SI*
145 *Appendix*, Fig. S1 *D* and *E*), suggesting that M1 has a specific enhancing role in fAβ
146 phagocytosis. To further examine the specificity of M1-mediated phagocytosis
147 enhancement, we conducted a similar experiment using two known phagocytosis
148 substrates, *Escherichia coli* (*E. coli*) and myelin debris. Notably, M1 failed to enhance
149 their uptake (Fig. 1 *H* and *I*). This finding indicates that M1 distinctly influences the
150 uptake mechanism of fAβ.
151
152 *Mode of action of M1*
153 GPR34 is a Gi/o-coupled GPCR that suppresses adenylyl cyclase and activates
154 downstream kinases such as AKT and ERK upon ligand binding (Fig. 2*A*). Consistent
155 with this, M1 treatment induced time-dependent increases in phosphorylated AKT and
156 ERK levels (*SI Appendix*, Fig. S2). We also investigated whether M1 alters cAMP levels.
157 To elevate the typically low steady-state cAMP levels, we pretreated cells with forskolin,
158 an activator of adenylyl cyclase. We then observed an expected rise in intracellular cAMP
159 concentration following forskolin treatment. However, when co-treated with M1, this
160 elevation in cAMP levels was counteracted (Fig. 2*B*). Considering that an elevated cAMP
161 level suppresses phagocytic activity (26–28), we investigated the effects on the fAβ
162 uptake in these treated cells. We found that the single treatment of forskolin was enough
163 to reduce the MFI of $fA\beta^+$ cells, while the co-treatment of M1 restored the impaired fAβ
164 uptake back to the basal level (Fig. 2*C*). Interestingly, forskolin specifically affect the
165 MFI without altering the proportion of $fA\beta^+$ cells like the effect of M1 (*SI Appendix*, Fig.
166 S3). Moreover, forskolin treatment did not alter the uptake of monomeric and oligomeric

167 Aβ species (Fig. 2 *D* and *E*). These data indicate that cAMP levels inversely correlate
168 with the phagocytic activity specifically for fAβ, which likely underlies the substrate-
169 specific effect of M1.
170
171 *M1 promotes microglial uptake of Aβ in vivo*
172 To explore the potential of M1 in promoting microglial uptake of Aβ *in vivo*, we
173 utilized the mutant *APP* knock-in $App^{NL\text{-}G\text{-}F}$ mouse model (hereafter NLGF mice) (29).
174 These mice, aged between 15–17 months, were administered a single injection of M1 into
175 the hippocampus. The next day, brain Aβ deposits were fluorescently labeled by
176 intraperitoneal injection of Methoxy-X04 (MX04). We then subjected these brains to flow
177 cytometry analysis of the CD11B+/CD45+ microglial population to quantify MX04-
178 positive cells (Fig. 3*A*). Our analysis revealed a notable increase in the MX04-positive
179 microglial fraction upon M1 administration (Fig. 3 *B* and *C*). This observation indicates
180 that M1 effectively enhances the microglial uptake of Aβ fibrils in an *in vivo* context.
181 Given that *Trem2* deficiency impairs Aβ metabolism in β-amyloidosis mice, this
182 receptor molecule is important for microglial recognition and uptake of Aβ. Consequently,
183 we asked whether the effect of M1 is somehow related to TREM2 function. For this
184 purpose, we employed *Tyrobp*-deficient mice (30), which lack a functional TREM2
185 receptor. We noted a significant reduction of MX04-positive microglia in *Tyrobp*-
186 deficient NLGF mice. Remarkably, M1 administration did not augment the MX04-
187 positive microglial fraction in these mice (Fig. 3*D*). These data suggest that M1's action
188 requires the function of TREM2/TYROBP in microglia.
189

190 *M1 promotes fAβ uptake by human iPSC-derived microglia-like cells*

191 Given the beneficial effect of M1 in promoting fAβ uptake by microglia, M1
192 emerges as a potential therapeutic candidate to boost fAβ metabolism in the brain. To
193 ascertain whether M1 exerts a comparable impact on human-derived microglia, we
194 employed a recently developed method for the efficient differentiation of microglia-like
195 cells (iMGLs) from human induced pluripotent stem cells (iPSCs) (Fig. 4*A*). This method
196 involves using iPSCs genetically modified to express the transcription factor *SPI1*, a
197 crucial factor for microglial differentiation (31). Implementing this protocol, we were able
198 to derive iMGLs exhibiting characteristic microglial projections (Fig. 4*B*). Subsequently,
199 we subjected these human iMGLs to the flow-cytometric analysis to assess the effect of
200 M1 on fAβ uptake (Fig. 4*C*). Notably, despite variations in the effective concentration
201 range, the stimulatory effect of M1 on fAβ uptake in human cells mirrored what we
202 observed in mouse primary microglia (Fig. 4*D*).

203

204 *Reduction of GPR34 expression in brain microglia associated with Alzheimer disease and*
205 *aging*

206 To investigate potential changes in GPR34 expression associated with AD, we
207 performed single-nucleus RNA-sequencing (snRNA-seq) on postmortem brains of 15
208 Japanese AD patients and 8 normal controls (*SI Appendix*, Table S1). We successfully
209 identified a distinct microglial cluster based on established marker genes (Fig. 5*A*).
210 *GPR34* expression was specifically enriched in this microglial population (Fig. 5*B*).
211 Notably, when comparing *GPR34* levels between AD patients and controls across the
212 annotated clusters, we observed a significant reduction in *GPR34* expression within the
213 microglial cluster from AD patients ($\log_2$FC = −0.49, adjusted p = 0.00004; Fig. 5*C*).

214 Among the differentially expressed genes between AD and control, *GPR34* ranked 311th.

215 To further characterize the microglial population (total 11,458 cells), we performed
216 subcluster analysis and identified 8 distinct subclusters (0–7) (Fig. 5*D*). The feature plot
217 of *GPR34* expression on the same UMAP space (Fig. 5*E*) suggested a relatively broad
218 expression across the subclusters, which was further detailed in the violin plot (Fig. 5*F*).
219 This plot revealed that *GPR34* expression was not prominently enriched in any specific
220 subcluster, except for subcluster 4, which exhibited significantly lower expression. When
221 comparing AD and control samples within each subcluster, a significant downregulation
222 of *GPR34* was observed in subcluster 0 ($\log_2$FC = −0.51, p = 0.0007). Although not
223 statistically significant, there was a trend towards decreased *GPR34* expression in the AD
224 group across other subclusters as well. Notably, subcluster 0, comprising 6,453 cells (56%
225 of the total) and being the largest subcluster, was characterized by the expression of
226 microglial genes such as *CSF1R* and *P2RY12*, suggesting that it represents homeostatic
227 microglia (*SI Appendix*, Fig. S4 *A* and *B*). On the other hand, subcluster 4, which exhibited
228 the lowest *GPR34* expression, was enriched for macrophage markers like *CD163*,
229 indicating its macrophage identity (*SI Appendix*, Fig. S4*C*). This finding is interesting
230 given that *GPR34* was previously identified as specifically expressed in microglia
231 compared to macrophages in mice (12). Our data suggest a similar specificity in humans.

232 To further support our findings, we reanalyzed publicly available AD snRNA-seq
233 datasets using the interactive web-based platform TACA (https://taca.lerner.ccf.org/),
234 specifically focusing on the study by Gerrits *et al.* (32). This dataset uniquely enabled the
235 dissection of Aβ and tau pathology contributions by including samples from the occipital
236 cortex (OC), which exhibits Aβ pathology but minimal tau pathology in AD, and the
237 occipitotemporal cortex (OTC) region, which harbors both Aβ and tau pathologies. This

238 analysis revealed that in the OC region, where only Aβ accumulation occurs, GPR34
239 expression was significantly reduced in microglia from both AD patients and healthy
240 controls with low-level Aβ pathology (CTR+) compared to pathology-free controls (*SI*
241 *Appendix*, Table S2 and Fig. S5). Intriguingly, in the OTC region affected by both Aβ and
242 tau pathologies, GPR34 levels were decreased in the CTR+ group with mild Aβ
243 accumulation, but paradoxically increased in the AD group exhibiting substantial tau
244 pathology. This suggests a potential differential effect of tau pathology on GPR34
245 expression, which warrants further investigation. Nonetheless, these findings corroborate
246 our observation of reduced GPR34 expression in microglia associated with Aβ pathology.
247 Next, we examined age-related changes in GPR34 expression using published
248 microglial RNA-seq datasets of both human and mouse origins. In humans, while Galatro
249 *et al.* (33) did not show significant age-dependent changes, Olah *et al.* (34) indicated a
250 substantial decrease ($\log_2$FC = −1.20, adjusted *p*-value = 0.044) in the aged population
251 compared to young individuals. In contrast, multiple mouse studies consistently revealed
252 a significant reduction in GPR34 levels in aged microglia compared to young adults (*SI*
253 *Appendix*, Fig. S6) (35–37), suggesting that an age-related decline in microglial GPR34
254 expression may be a conserved phenomenon across species.
255 The concordant findings from human AD and aging mouse models highlight a
256 common pattern of decreased microglial GPR34 expression, which could impair Aβ
257 clearance capability. This age-related reduction in GPR34 levels/activity may contribute
258 to Aβ accumulation in the aging brain and exacerbate AD pathogenesis. Collectively,
259 these results underscore the importance of maintaining or enhancing microglial GPR34
260 activity, for which GPR34 agonists represent a potential therapeutic strategy to promote
261 effective Aβ clearance and prevent pathological Aβ accumulation.
262

263 **Discussion**

264 In this study, we identified the G protein-coupled receptor GPR34 as a key regulator
265 of microglial phagocytosis of Aβ fibrils. Activating GPR34 with a selective agonist, M1,
266 significantly enhances the phagocytosis of Aβ fibrils in both mouse and human microglia,
267 highlighting the translational potential of targeting GPR34 for promoting Aβ clearance.
268 Importantly, a single intrahippocampal injection of M1 in a β-amyloidosis mouse model
269 substantially increased microglial phagocytosis of Aβ, providing compelling evidence for
270 the *in vivo* efficacy of GPR34 activation. Mechanistically, M1 suppresses intracellular
271 cAMP levels, which inversely correlate with microglial Aβ phagocytosis activity,
272 suggesting that GPR34-mediated cAMP signaling plays a crucial role in regulating Aβ
273 clearance. Furthermore, transcriptomic analyses revealed a significant reduction in
274 *GPR34* expression associated with AD pathology, indicating that decreased GPR34 levels
275 may contribute to impaired Aβ clearance and disease progression. Collectively, our
276 findings establish GPR34 as a promising therapeutic target for AD and underscore the
277 potential of GPR34 agonists as a novel strategy to promote Aβ clearance and mitigate AD
278 pathogenesis.

279 The inverse correlation between cAMP levels and fAβ phagocytosis is consistent
280 with previous reports demonstrating the inhibitory role of cAMP in phagocytosis (26–28).
281 These studies suggest that elevated cAMP levels can suppress phagocytic activity,
282 possibly by modulating key signaling pathways or cytoskeletal reorganization processes
283 involved in particle engulfment. Interestingly, the selective impact of M1/forskolin on
284 fAβ uptake, but not on the internalization of soluble Aβ species, aligns with the notion
285 that distinct mechanisms govern the uptake of different Aβ forms (25). On the other hand,
286 the reason why M1 did not affect the uptake of myelin or *E. coli* particles, which are also

287 internalized through phagocytosis, remains unclear. However, it is possible that cAMP
288 exerts selective effects on Aβ receptors. In this regard, it is particularly intriguing that M1
289 failed to augment Aβ uptake in *Tyrobp*-deficient mice, which lack functional TREM2.
290 Given the established role of TREM2 in mediating microglial phagocytosis of Aβ, it is
291 plausible that GPR34 activation may modulate TREM2-dependent fAβ uptake by
292 regulating cAMP signaling. However, further investigation is needed to elucidate the
293 precise molecular mechanisms underlying this interaction. Furthermore, the Aβ fibrils
294 used in this study form larger aggregates compared to myelin and *E. coli*, and the
295 molecular mechanisms of phagocytosis are known to differ depending on the target size
296 (38). Thus, these substrates may be internalized through distinct pathways with varying
297 sensitivity to cAMP regulation.

298 cAMP has been implicated in the regulation of various microglial functions (39, 40).
299 Interestingly, microglia express several Gi/o-coupled receptors, including GPR34,
300 P2RY12, P2RY13, CX3CR1, and GPR84 (12), but the functional significance of this
301 apparent redundancy remains elusive. While it is natural to assume that these receptors
302 converge on the same cellular response due to the rapid diffusion of cAMP, evidence
303 suggests that cAMP and its metabolic enzymes can be localized beneath phagocytic cups
304 (41, 42), and cAMP can form spatially restricted signaling compartments (43). This
305 compartmentalization raises the possibility that GPR34 and other Gi/o-coupled receptors
306 may regulate distinct pools of cAMP with unique functional consequences, such as
307 modulating fAβ phagocytosis. Future studies aimed at dissecting the spatial and
308 functional organization of cAMP signaling in microglia will be crucial to understanding
309 the specific roles of these receptors in microglial function and AD pathogenesis.

310 Our snRNA-seq analysis of a Japanese AD patient cohort and reanalysis of the

311 Gerrits dataset consistently revealed a significant reduction in *GPR34* expression in AD
312 microglia, in agreement with previously published data (32, 44). Intriguingly, the Gerrits
313 dataset suggests that this reduction is more closely associated with Aβ accumulation than
314 with tau pathology. In contrast, experimental studies using β-amyloidosis mouse models,
315 such as the APP/PS1 (45, 46) and NLGF mice (47), have reported increased *Gpr34*
316 expression in microglia. While this discrepancy between human and mouse data could be
317 attributed to species-specific differences in GPR34 regulation, an alternative explanation
318 may lie in the age-dependent decline of GPR34 expression observed in both human and
319 mouse datasets. Interestingly, a similar age-associated decrease has been reported for
320 another microglial gene, *Cd22*, which impairs phagocytic activity (35). We hypothesize
321 that the age-related reduction in *GPR34* levels may contribute to impaired Aβ clearance
322 and increased Aβ accumulation in the aging brain, potentially increasing the risk of
323 developing AD. However, the further decrease in *GPR34* expression observed in AD
324 patients compared to controls suggests that additional factors, such as genetic
325 predisposition, may exacerbate *GPR34* downregulation in AD. The precise mechanisms
326 underlying the downregulation of *GPR34* remain elusive; however, our findings
327 underscore the potential significance of this process in AD pathogenesis and highlight the
328 complex interplay between *GPR34* expression, aging, and AD pathology.

329 While M1 is a promising compound for promoting microglial Aβ phagocytosis, its
330 structure suggests limited blood-brain barrier permeability, necessitating direct brain
331 administration in this study and precluding a thorough evaluation of long-term efficacy.
332 The development of orally bioavailable GPR34 agonists with improved brain penetrance
333 would enable more comprehensive investigations into the therapeutic potential of GPR34
334 activation in AD models. In this regard, our recent elucidation of the GPR34-M1 binding

335 structure (19) may facilitate the rational design of novel GPR34 agonists. However, it is
336 also important to consider potential side effects related to GPR34's roles in immune
337 regulation and neuropathic pain (24). Future studies should carefully examine the safety
338 and tolerability of novel GPR34 agonists in preclinical AD models.

339 In summary, our findings identify GPR34 as a novel therapeutic target for enhancing
340 microglial phagocytosis of Aβ and highlight the potential of GPR34 agonists as a disease-
341 modifying strategy for AD. Further research into the development of potent GPR34
342 agonists and their long-term safety and efficacy could lead to novel therapeutic
343 approaches for this devastating disorder.

344

345 **Materials and methods**

346

347 Full methods are available in *SI Appendix, Supplementary Methods*.

348

349 Mice

350 All animal procedures were conducted in accordance with the protocols approved
351 by the Institutional Animal Care and Use Committee at the University of Tokyo (UT)
352 (protocol no. P5-04). See *SI Appendix* for further details.

353

354 Aβ uptake assay in primary microglia

355 Primary microglia were prepared from neonatal C57BL/6J mice as described
356 previously (48). For the Aβ uptake assay, cells were serum-starved in DMEM for 30 min
357 and then treated with fluorescently labeled Aβ species (monomer, oligomer, or fibril) and
358 either M1 or vehicle in DMEM containing 1% FBS for 3 hours. Cells were then detached,
359 and for experiments involving Aβ oligomers or fibrils, the cell suspension was mixed with
360 trypan blue solution to quench any extracellular fluorescence. The internalized Aβ

361 fluorescence was quantified using flow cytometry. Data were normalized to the MFI of
362 control cells treated with fAβ alone (i.e., without M1 or vehicle treatment). See *SI*
363 *Appendix* for further details.
364
365 Differentiation of Human Induced Pluripotent Stem Cell-derived Microglia and Aβ Uptake
366 Assay
367 Microglia-like cells were differentiated from human induced pluripotent stem cells
368 (iPSCs) using a previously described protocol (31). Briefly, iPSCs were genetically
369 engineered to express the transcription factor *SPI1* under a doxycycline-inducible system.
370 The differentiated microglia-like cells were used for Aβ uptake assays, where they were
371 treated with fluorescently labeled Aβ fibrils and M1 for 4.5 hours. The internalized Aβ
372 fluorescence was quantified using flow cytometry. See *SI Appendix* for further details.
373
374 Stereotaxic injection of M1 and measurement of microglial uptake of Aβ *in vivo*
375 To assess the effect of M1 on microglial uptake of Aβ *in vivo*, 15–17-month-old male
376 and female NLGF mice were used. Mice were anesthetized, and 0.8 μL of 250 μM M1
377 was injected into one hippocampus, while an equal volume of vehicle was injected into
378 the contralateral hippocampus using stereotaxic coordinates. Nine hours after M1
379 injection, mice were administered methoxy-X04 intraperitoneally (MX04) to label Aβ
380 fibrils *in vivo*. Three hours later, mice were perfused, and the hippocampi were dissected.
381 Microglial cells were isolated and the percentage of MX04-positive microglia (CD11B+
382 CD45+ PI−) was assessed by flow cytometry. See *SI Appendix* for further details.
383
384 Human samples
385 Autopsied human brain tissues from 15 AD patients and 8 controls without

386 neurodegenerative pathology (Table S1) were obtained from the Brain Bank for Aging
387 Research via the Japan Brain Bank Net. Written informed consent was obtained from the
388 family of the deceased. Dissected brain tissues were quickly frozen with dry ice powder
389 and stored at −80°C. Single-nucleus RNA sequencing (snRNA-seq) analysis was
390 performed at Niigata University (NU) using frontal cortex samples. This research was
391 approved by the Ethics Committees of the Tokyo Metropolitan Institute for Geriatrics and
392 Gerontology (TMIG) (permit number: OF-23), NU (G2018-0034), and the UT (5-15).
393
394 Isolation of nuclei and single-nucleus RNA sequencing
395 Nuclei were isolated from fresh frozen postmortem brain tissue, and for each sample,
396 approximately 10,000 nuclei were processed for snRNA-seq using the Chromium Next
397 GEM Single Cell 3' Kit v3.1 (10x Genomics). Raw sequencing data were processed using
398 the Cell Ranger pipeline (v7.0.0, 10x Genomics) for demultiplexing, barcode assignment,
399 read alignment to the human reference genome (GRCh38-2020-A), and gene counting.
400 Subsequent analysis was performed by using the R package *Seurat* (v5.0.1). See *SI*
401 *Appendix* for further details.
402
403 Tools and resources used in the preparation of this work
404 The authors employed Anthropic's Claude for assistance in revising and refining the
405 manuscript. After using this tool, the authors reviewed and edited the content as needed
406 and take full responsibility for the content of the publication. Illustrations were created
407 with BioRender.com. Chemical structures were generated using Marvin (Chemaxon).
408
409 Statistical analysis
410 Statistical analyses and graphical presentations were performed using GraphPad

411 Prism 10. The specific statistical tests used and sample sizes for each experiment are
412 indicated in the corresponding figure legends. P-values lower than 0.05 were considered
413 statistically significant, except for the snRNA-seq analysis, and are represented by
414 asterisks: *$p < 0.05$, **$p < 0.01$, ***$p < 0.001$, ****$p < 0.0001$. Non-significant
415 differences ($p > 0.05$) are indicated by "ns".
416

Data, Materials, and Software Availability

The snRNA-seq data generated in this study are currently being prepared for the deposition in the DNA Data Bank of Japan (DDBJ; https://www.ddbj.nig.ac.jp/index.html). All other data are included in the manuscript and/or supporting information.

Acknowledgments

This work was supported by the JSPS Grants-in-Aid for Scientific Research (KAKENHI) under grant numbers 19H01015, 23H00394 (to T. Tomita), 19K07080, 22K07344 (to S.T.), 21H05633 (to H.W.), 21K07271 (to A.M.), and 22H04923 (CoBiA) (to Y.S. and S.M.); AMED under grant numbers JP22dm0207072 (to T. Tomita), JP22dm0207073 (to T. Tomita and S.T.), JP21bm0804003, JP23bm1123046, JP23kk0305024 (to H.O.), JP23wm0525019 (to M.K. and T.I.), JP24dk0207060 (to T.I., A.M., and M.K.), and JP21wm0425019 (to Y.S. and S.M.); JST Moonshot R&D under grant number JPMJMS2024 (to T. Tomita); Integrated Research Initiative for Living Well with Dementia (IRIDE) of the TMIG (to Y.S. and S.M.); MHLW Research on rare and intractable diseases Program Grant Number JPMH23FC1008 (to Y.S.); ONO Medical Research Foundation (to S.T.). We would like to thank Dr. Shinya Yamanaka (Kyoto University) for the kind gifts of the 201B7 iPSC line.

Author Contributions

Conceptualization, S.T., J.A., and T. Tomita; Methodology, S.T., W.W., H.E, I.S., H.W., H.O., N.H., A.M., M.K., and T.I.; Investigation, H.E., N.H., M.H., A.A., and J.O.; Resources, T.O., J.A., M.M., Y.S., S.M., A.M., T.I., H.W., H.O., T. S., T.C.S, and T. Takai; Writing – Original Draft, S.T. and H.E.; Review & Editing, S.T.; Project Administration,

S.T., H.W. and A.M.; Supervision, S.T., T. Tomita, J.A., H.O., and I.T.

Competing interests

H. Okano is a scientific consultant for SanBio, Co. Ltd., and K Pharma Inc. The other authors declare neither financial nor non-financial competing interests.

References

1. D. J. Selkoe, J. Hardy, The amyloid hypothesis of Alzheimer's disease at 25 years. *EMBO Mol Med* **8**, 595–608 (2016).
2. T. Jonsson, *et al.*, A mutation in APP protects against Alzheimer's disease and age-related cognitive decline. *Nature* **488**, 96–9 (2012).
3. J. Sevigny, *et al.*, The antibody aducanumab reduces Aβ plaques in Alzheimer's disease. *Nature* **537**, 50–6 (2016).
4. C. H. van Dyck, *et al.*, Lecanemab in Early Alzheimer's Disease. *N Engl J Med* **388**, 9–21 (2023).
5. D. V Hansen, J. E. Hanson, M. Sheng, Microglia in Alzheimer's disease. *J Cell Biol* **217**, 459–472 (2018).
6. S. Takatori, W. Wang, A. Iguchi, T. Tomita, Genetic Risk Factors for Alzheimer Disease: Emerging Roles of Microglia in Disease Pathomechanisms. *Adv Exp Med Biol* **1118**, 83–116 (2019).
7. T. Jonsson, *et al.*, Variant of TREM2 associated with the risk of Alzheimer's disease. *N Engl J Med* **368**, 107–16 (2013).
8. R. Guerreiro, *et al.*, TREM2 variants in Alzheimer's disease. *N Engl J Med* **368**, 117–27 (2013).
9. Y. Wang, *et al.*, TREM2 lipid sensing sustains the microglial response in an Alzheimer's disease model. *Cell* **160**, 1061–71 (2015).
10. T. R. Jay, *et al.*, Disease Progression-Dependent Effects of TREM2 Deficiency in a Mouse Model of Alzheimer's Disease. *J Neurosci* **37**, 637–647 (2017).
11. S. Parhizkar, *et al.*, Loss of TREM2 function increases amyloid seeding but reduces plaque-associated ApoE. *Nat Neurosci* **22**, 191–204 (2019).
12. M. L. Bennett, *et al.*, New tools for studying microglia in the mouse and human CNS. *Proc Natl Acad Sci U S A* **113**, E1738-46 (2016).
13. S. Krasemann, *et al.*, The TREM2-APOE Pathway Drives the Transcriptional Phenotype of Dysfunctional Microglia in Neurodegenerative Diseases. *Immunity* **47**, 566-581.e9 (2017).
14. T. Sugo, *et al.*, Identification of a lysophosphatidylserine receptor on mast cells. *Biochem Biophys Res Commun* **341**, 1078–87 (2006).
15. A. Inoue, *et al.*, TGFα shedding assay: an accurate and versatile method for detecting GPCR activation. *Nat Methods* **9**, 1021–9 (2012).
16. H. Kitamura, *et al.*, GPR34 is a receptor for lysophosphatidylserine with a fatty acid at the sn-2 position. *J Biochem* **151**, 511–8 (2012).
17. A. Uwamizu, *et al.*, Lysophosphatidylserine analogues differentially activate three

484 LysoPS receptors. *J Biochem* **157**, 151–60 (2015).
485 18. S. Nakamura, *et al.*, Non-naturally Occurring Regio Isomer of Lysophosphatidylserine
486 Exhibits Potent Agonistic Activity toward G Protein-Coupled Receptors. *J Med Chem*
487 **63**, 9990–10029 (2020).
488 19. T. Izume, *et al.*, Structural basis for lysophosphatidylserine recognition by GPR34. *Nat*
489 *Commun* **15**, 902 (2024).
490 20. I. Liebscher, *et al.*, Altered immune response in mice deficient for the G protein-
491 coupled receptor GPR34. *J Biol Chem* **286**, 2101–10 (2011).
492 21. E. Jäger, *et al.*, Dendritic Cells Regulate GPR34 through Mitogenic Signals and
493 Undergo Apoptosis in Its Absence. *J Immunol* **196**, 2504–13 (2016).
494 22. X. Wang, *et al.*, GPR34-mediated sensing of lysophosphatidylserine released by
495 apoptotic neutrophils activates type 3 innate lymphoid cells to mediate tissue repair.
496 *Immunity* **54**, 1123-1136.e8 (2021).
497 23. J. Preissler, *et al.*, Altered microglial phagocytosis in GPR34-deficient mice. *Glia* **63**,
498 206–15 (2015).
499 24. A. Sayo, *et al.*, GPR34 in spinal microglia exacerbates neuropathic pain in mice. *J*
500 *Neuroinflammation* **16**, 82 (2019).
501 25. S. Mandrekar, *et al.*, Microglia Mediate the Clearance of Soluble Aβ through Fluid
502 Phase Macropinocytosis. *The Journal of Neuroscience* **29**, 4252–4262 (2009).
503 26. D. M. Aronoff, C. Canetti, M. Peters-Golden, Prostaglandin E2 inhibits alveolar
504 macrophage phagocytosis through an E-prostanoid 2 receptor-mediated increase in
505 intracellular cyclic AMP. *J Immunol* **173**, 559–65 (2004).
506 27. S. A. Kalamidas, *et al.*, cAMP synthesis and degradation by phagosomes regulate actin
507 assembly and fusion events: consequences for mycobacteria. *J Cell Sci* **119**, 3686–94
508 (2006).
509 28. C. H. Serezani, *et al.*, Prostaglandin E2 suppresses bacterial killing in alveolar
510 macrophages by inhibiting NADPH oxidase. *Am J Respir Cell Mol Biol* **37**, 562–70
511 (2007).
512 29. T. Saito, *et al.*, Single App knock-in mouse models of Alzheimer's disease. *Nat*
513 *Neurosci* **17**, 661–3 (2014).
514 30. T. Kaifu, *et al.*, Osteopetrosis and thalamic hypomyelinosis with synaptic degeneration
515 in DAP12-deficient mice. *J Clin Invest* **111**, 323–32 (2003).
516 31. I. Sonn, *et al.*, Single transcription factor efficiently leads human induced pluripotent
517 stem cells to functional microglia. *Inflamm Regen* **42**, 20 (2022).
518 32. E. Gerrits, *et al.*, Distinct amyloid-β and tau-associated microglia profiles in
519 Alzheimer's disease. *Acta Neuropathol* **141**, 681–696 (2021).

33. T. F. Galatro, *et al.*, Transcriptomic analysis of purified human cortical microglia reveals age-associated changes. *Nat Neurosci* **20**, 1162–1171 (2017).
34. M. Olah, *et al.*, A transcriptomic atlas of aged human microglia. *Nat Commun* **9**, 539 (2018).
35. J. V Pluvinage, *et al.*, CD22 blockade restores homeostatic microglial phagocytosis in ageing brains. *Nature* **568**, 187–192 (2019).
36. A. L. Thomas, M. A. Lehn, E. M. Janssen, D. A. Hildeman, C. A. Chougnet, Naturally-aged microglia exhibit phagocytic dysfunction accompanied by gene expression changes reflective of underlying neurologic disease. *Sci Rep* **12**, 19471 (2022).
37. S. R. Ocañas, *et al.*, Microglial senescence contributes to female-biased neuroinflammation in the aging mouse hippocampus: implications for Alzheimer's disease. *J Neuroinflammation* **20**, 188 (2023).
38. D. Schlam, *et al.*, Phosphoinositide 3-kinase enables phagocytosis of large particles by terminating actin assembly through Rac/Cdc42 GTPase-activating proteins. *Nat Commun* **6**, 8623 (2015).
39. L.-P. Bernier, *et al.*, Nanoscale Surveillance of the Brain by Microglia via cAMP-Regulated Filopodia. *Cell Rep* **27**, 2895-2908.e4 (2019).
40. M. Merlini, *et al.*, Microglial Gi-dependent dynamics regulate brain network hyperexcitability. *Nat Neurosci* **24**, 19–23 (2021).
41. K. B. Pryzwansky, A. L. Steiner, J. K. Spitznagel, C. L. Kapoor, Compartmentalization of cyclic AMP during phagocytosis by human neutrophilic granulocytes. *Science* **211**, 407–10 (1981).
42. M. N. Ballinger, T. Welliver, S. Straight, M. Peters-Golden, J. A. Swanson, Transient increase in cyclic AMP localized to macrophage phagosomes. *PLoS One* **5**, e13962 (2010).
43. J. Z. Zhang, *et al.*, Phase Separation of a PKA Regulatory Subunit Controls cAMP Compartmentation and Oncogenic Signaling. *Cell* **182**, 1531-1544.e15 (2020).
44. S. Morabito, *et al.*, Single-nucleus chromatin accessibility and transcriptomic characterization of Alzheimer's disease. *Nat Genet* **53**, 1143–1155 (2021).
45. N. Ma, *et al.*, Whole-Transcriptome Analysis of APP/PS1 Mouse Brain and Identification of circRNA-miRNA-mRNA Networks to Investigate AD Pathogenesis. *Mol Ther Nucleic Acids* **18**, 1049–1062 (2019).
46. L.-L. Lin, *et al.*, GPR34 Knockdown Relieves Cognitive Deficits and Suppresses Neuroinflammation in Alzheimer's Disease via the ERK/NF-κB Signal. *Neuroscience* **528**, 129–139 (2023).
47. A. Sobue, *et al.*, Microglial gene signature reveals loss of homeostatic microglia

associated with neurodegeneration of Alzheimer's disease. *Acta Neuropathol Commun* **9**, 1 (2021).

48. Y. Kato, *et al.*, Protocol for gene knockdown using siRNA in primary cultured neonatal murine microglia. *STAR Protoc* **5**, 102867 (2024).

562 **Figure legends**

563 Fig.1: GPR34-selective agonist M1 specifically increased fibrillar Aβ uptake by murine
564 primary microglia

565 (***A***) The chemical structure of the GPR34 agonist M1. (***B***) Representative flow cytometry
566 plots showing uptake of fluorescently labeled Aβ fibrils (fAβ) by mouse primary
567 microglia pretreated with 10 nM M1 or vehicle, after 3-hours incubation with fAβ. (***C***)
568 M1 increased the mean fluorescence intensity (MFI) of fAβ+ cells in a concentration-
569 dependent manner after 3 hours of fAβ treatment. Data are normalized to the MFI of
570 control cells treated with fAβ alone (*i.e.*, without M1 or vehicle treatment) (N=4;
571 Dunnett's test). (***D***) Time course analysis showing the effect of 10 nM M1 on fAβ uptake
572 by microglia (N=7–8; paired t-test). (***E***) Knockdown efficiencies of two independent
573 *Gpr34* siRNAs were validated by RT-qPCR (N=3, Dunnett's test). (***F***) The M1-mediated
574 increase in fAβ uptake was abolished by *Gpr34* knockdown using these siRNAs (N=5–
575 6; two-way repeated measures ANOVA followed by Šídák's multiple comparisons test).
576 ***G–I*** M1 did not affect microglial uptake of fluorescently labeled Aβ monomers or
577 oligomers (***G***, N=3, Dunnett's test), *E. coli* particles (***H***, N=5, paired t-test) or myelin
578 debris (***I***, N=3, paired t-test). Bars represent the mean ± SEM.

579

580 Fig.2: M1 reduces intracellular concentration of cAMP

581 (***A***) Schematic illustrating the proposed mechanism by which GPR34 activation reduces
582 intracellular cAMP levels. (***B***) Treatment with the adenylyl cyclase (AC) activator
583 forskolin increased intracellular cAMP levels in primary microglia, which was
584 counteracted by co-treatment with 10 nM M1 (N=5, one-way repeated measures ANOVA
585 and Tukey's test). ***C–E*** Forskolin treatment suppressed microglial uptake of fAβ. This

586 impairment was rescued by co-treatment with M1 (***C***, N=6, one-way repeated measures
587 ANOVA and Tukey's test). In contrast, forskolin did not significantly affect microglial
588 uptake of monomeric (***D***) or oligomeric (***E***) Aβ species (N=3, paired t-test). Bars represent
589 the mean ± SEM.
590
591 Fig.3: The effect of M1 on microglial uptake of Aβ fibrils *in vivo*
592 (***A***) Experimental design schematic. 15–17 month-old male and female NLGF mice
593 received bilateral intrahippocampal injections of vehicle or M1 (250 μM, 0.8 μL),
594 followed by intraperitoneal injection of the Aβ tracer Methoxy-X04 (MX04; 10 mg/kg)
595 the next day. Hippocampi were harvested 12 hours after M1 injection for flow cytometry
596 analysis of MX04+ microglia (CD11B+/CD45+). ***B***, ***C*** Representative flow cytometry
597 plots (***B***) and quantification (***C***) showing an increase in the percentage of MX04+
598 microglia upon M1 administration. (***D***) In *Tyrobp*-deficient NLGF mice lacking
599 functional TREM2, M1 failed to increase the percentage of MX04+ microglia. Each pair
600 of data points connected by a line represents a single experiment (N=6; male and female
601 mice are indicated in *green* and *magenta*, respectively). Bars represent the mean ± SEM.
602 Paired t-test.
603
604 Fig.4: The effect of M1 in human iPSC-derived microglia-like cells
605 (***A***) Protocol for differentiating human iPSC-derived microglia-like cells (iMGLs) using
606 a doxycycline (DOX)-inducible SPI1 expression system.
607 (***B***) A representative image of human iPSC-derived microglia-like cells (Scale bar: 100
608 μm). ***C***, ***D*** Representative flow cytometry plots (***C***) and quantification (***D***) showing an
609 increase in fAβ uptake by microglia upon M1 treatment (N=7). Bars represent the mean
610 ± SEM. Dunnett's test.

611

612 Fig.5: Reduced *GPR34* expression in microglia associated with Alzheimer disease

613 ***A***–***C*** snRNA-seq analysis of the frontal cortex from 15 AD patients and 8 controls in the

614 Japanese cohort. UMAP visualization of major cell types (***A***). Feature plot showing the

615 expression of *GPR34* (***B***). Violin plots depicting the expression of *GPR34* in microglia

616 (***C***). A significant reduction in *GPR34* expression was observed in AD microglia

617 compared to controls ($\log_2$FC = −0.49, adjusted p = 0.00004). ***D***–***F*** Subcluster analysis

618 of the microglial population. UMAP visualization of microglial subclusters (0-7)

619 identified by unsupervised clustering of the microglial population from panel ***A*** (***D***).

620 Feature plot showing the expression of *GPR34* (***E***). Violin plots depicting the expression

621 of GPR34 in each microglial subcluster (***F***).

622

Figure 1

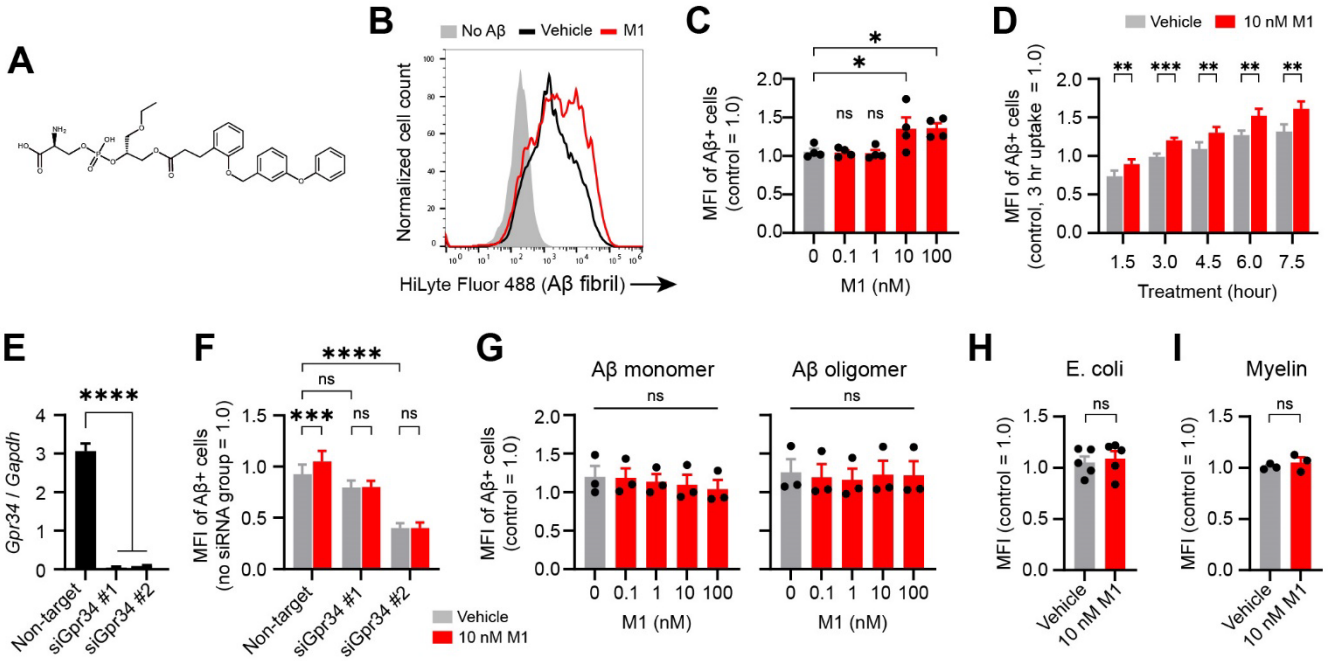
A
B
No Aβ
Vehicle
M1
Normalized cell count
HiLyte Fluor 488 (Aβ fibril)
C
MFI of Aβ+ cells (control = 1.0)
M1 (nM)
D
Vehicle
10 nM M1
MFI of Aβ+ cells (control, 3 hr uptake = 1.0)
Treatment (hour)
E
Gpr34 / Gapdh
Non-target
siGpr34 #1
siGpr34 #2
F
MFI of Aβ+ cells (no siRNA group = 1.0)
Vehicle
10 nM M1
G
Aβ monomer
Aβ oligomer
MFI of Aβ+ cells (control = 1.0)
M1 (nM)
H
E. coli
MFI (control = 1.0)
I
Myelin
MFI (control = 1.0)

Figure 2

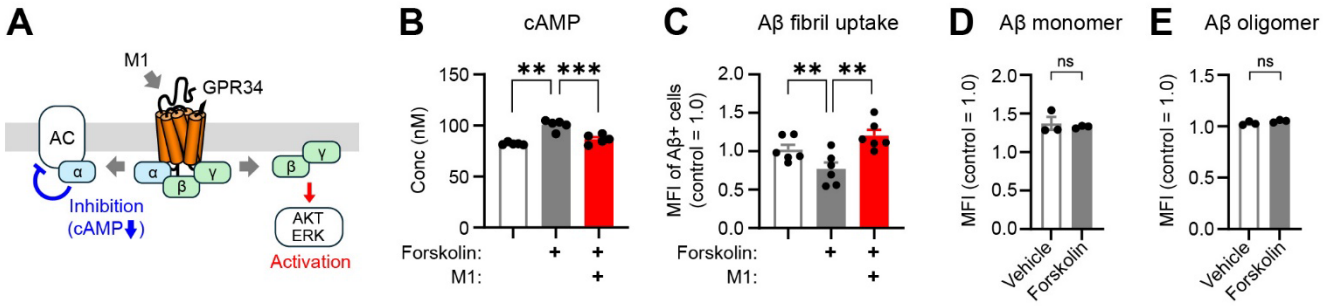
A
M1
GPR34
AC
α
α
β
γ
β
γ
Inhibition
(cAMP↓)
AKT
ERK
Activation
B
cAMP
Conc (nM)
150
100
50
0
**
***
Forskolin:
M1:
C
Aβ fibril uptake
MFI of Aβ+ cells
(control = 1.0)
2.0
1.5
1.0
0.5
0.0
**
**
Forskolin:
M1:
D
Aβ monomer
MFI (control = 1.0)
ns
Vehicle
Forskolin
E
Aβ oligomer
MFI (control = 1.0)
ns
Vehicle
Forskolin

Figure 3

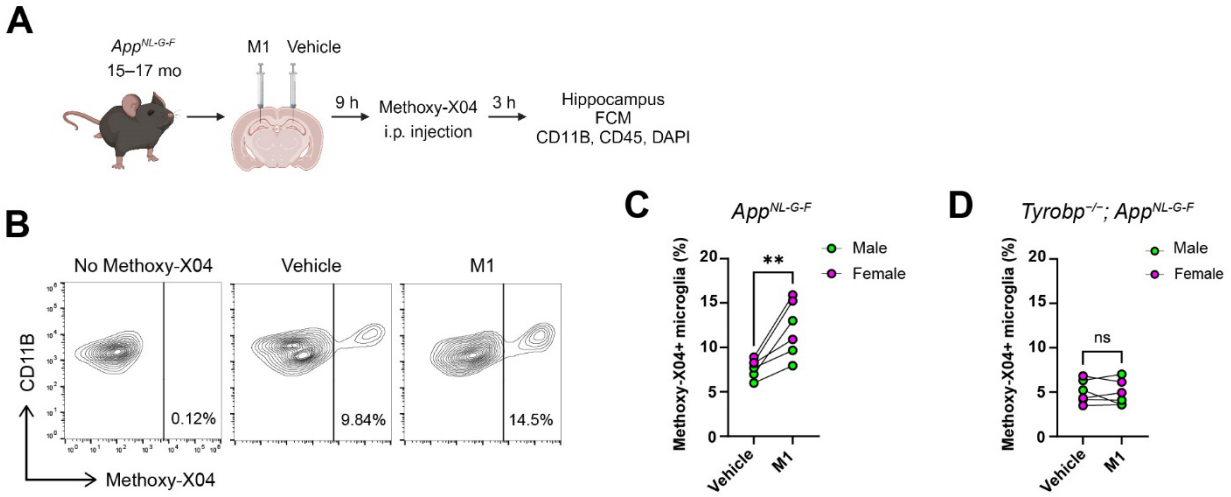
A
App^NL-G-F
15–17 mo
M1
Vehicle
9 h
Methoxy-X04
i.p. injection
3 h
Hippocampus
FCM
CD11B, CD45, DAPI
B
No Methoxy-X04
Vehicle
M1
CD11B
Methoxy-X04
0.12%
9.84%
14.5%
C
App^NL-G-F
Methoxy-X04+ microglia (%)
**
Male
Female
Vehicle
M1
D
Tyrobp^-/-; App^NL-G-F
Methoxy-X04+ microglia (%)
ns
Male
Female
Vehicle
M1

Figure 4

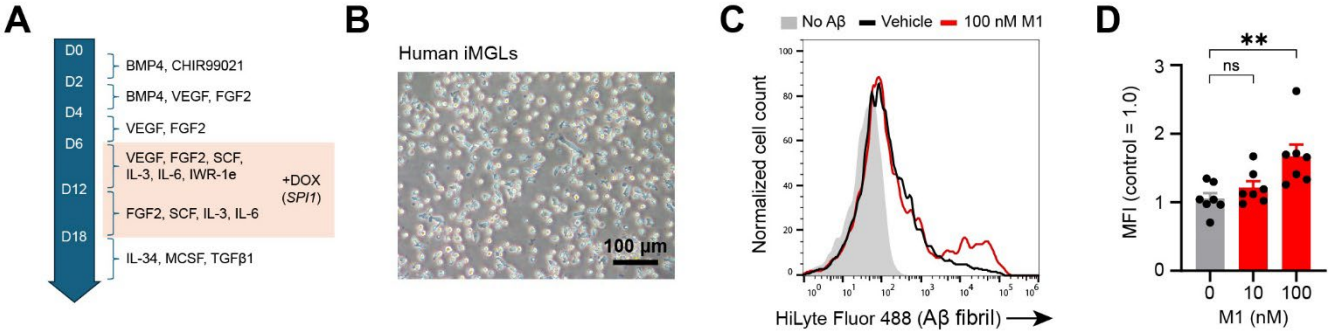
A
D0
D2
D4
D6
D12
D18
BMP4, CHIR99021
BMP4, VEGF, FGF2
VEGF, FGF2
VEGF, FGF2, SCF, IL-3, IL-6, IWR-1e
FGF2, SCF, IL-3, IL-6
+DOX (SPI1)
IL-34, MCSF, TGFβ1
B
Human iMGLs
100 µm
C
No Aβ
Vehicle
100 nM M1
Normalized cell count
HiLyte Fluor 488 (Aβ fibril)
D
MFI (control = 1.0)
ns
**
0
10
100
M1 (nM)

Figure 5

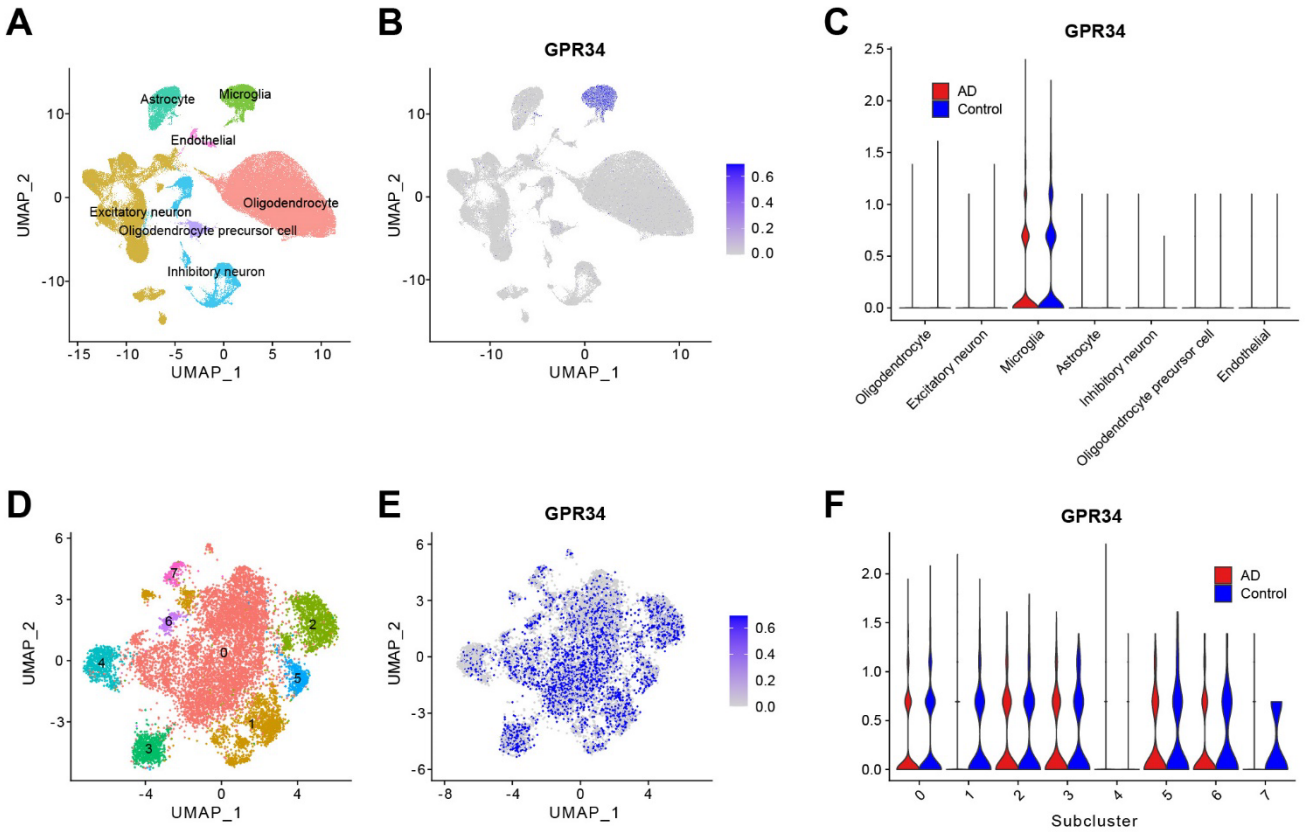
A
Astrocyte
Microglia
Endothelial
Oligodendrocyte
Excitatory neuron
Oligodendrocyte precursor cell
Inhibitory neuron
UMAP_2
UMAP_1
B
GPR34
C
GPR34
AD
Control
Oligodendrocyte
Excitatory neuron
Microglia
Astrocyte
Inhibitory neuron
Oligodendrocyte precursor cell
Endothelial
D
E
GPR34
F
GPR34
Subcluster